View Article Online
View Journal

ChemComm

Accepted Manuscript

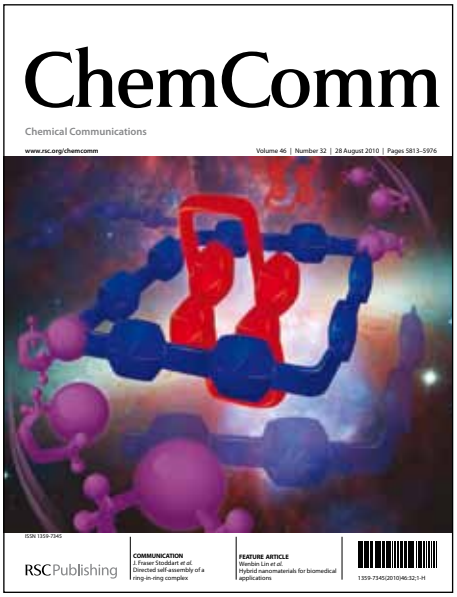

This is an *Accepted Manuscript*, which has been through the RSC Publishing peer review process and has been accepted for publication.

Accepted Manuscripts are published online shortly after acceptance, which is prior to technical editing, formatting and proof reading. This free service from RSC Publishing allows authors to make their results available to the community, in citable form, before publication of the edited article. This *Accepted Manuscript* will be replaced by the edited and formatted *Advance Article* as soon as this is available.

To cite this manuscript please use its permanent Digital Object Identifier (DOI®), which is identical for all formats of publication.

More information about *Accepted Manuscripts* can be found in the **Information for Authors**.

Please note that technical editing may introduce minor changes to the text and/or graphics contained in the manuscript submitted by the author(s) which may alter content, and that the standard **Terms & Conditions** and the **ethical guidelines** that apply to the journal are still applicable. In no event shall the RSC be held responsible for any errors or omissions in these *Accepted Manuscript* manuscripts or any consequences arising from the use of any information contained in them.

ChemComm

Dynamic Article Links ►
View Article Online

Cite this: DOI: 10.1039/c0xx00000x

www.rsc.org/xxxxxx

COMMUNICATION

Ultra-stable CdS Incorporated Ti-MCM-48 Mesoporous Materials for Efficient Photocatalytic Decomposition of Water under Visible Light Illumination

*Rui Peng[a], Chia-Ming Wu[a], Jonas Baltrusaitis[b], Nada M. Dimitrijevic[c], Tijana Rajh[c] and, Ranjit T. Koodali[a]**

Received (in XXX, XXX) Xth XXXXXXXXX 20XX, Accepted Xth XXXXXXXXX 20XX
DOI: 10.1039/b000000x

Downloaded by Dalian Institute of Chemical Physics, CAS on 12 March 2013
Published on 27 February 2013 on http://pubs.rsc.org | doi:10.1039/C3CC41362D

Chemical Communications Accepted Manuscript

A RuO_2-CdS-Ti-MCM-48 mesoporous material has been prepared. This composite material generates hydrogen and oxygen in the absence of Pt co-catalyst and most importantly photocorrosion of CdS is completely eliminated.

Photocatalytic cleavage of water has been acknowledged as a clean means to generate hydrogen and oxygen to alleviate the impact of fossil fuels and address global environmental issues. The photoelectrochemical splitting of water was originally realized by Fujishima and Honda under UV illumination.[1] Inspired by this work, extensive efforts have been devoted and a myriad of semiconductors have been explored.[2-4] The large bandgap energies of most semiconductors necessitate the use of UV light, which constitutes ~ 5% of the solar spectrum Therefore, to enhance photocatalytic efficiencies and make better use of solar energy, photocatalysts that can harness visible light effectively are essential.

CdS has been explored extensively in photocatalysis.[5] However, a big drawback of CdS is its propensity to undergo photocorrosion.[6] Efforts to alleviate this include use of sulfide/ sulfite as sacrificial electron donor/agents, deposition of noble metals, incorporation of CdS in porous materials and preparing coupled semiconductors.[5, 7, 8] Confinement of CdS clusters in porous supports provide advantages such as: i) high dispersion of the semiconductor material that affords several catalytic sites per nm^2, ii) enhanced stability towards photocorrosion since less surface area of CdS is exposed, and iii) limiting the size of CdS due to quantum confinement that shifts the conduction band (c.b.) edge to more negative values. The small size of the semiconductor enables fast diffusion of charge-carriers to the surface active sites thus minimizing the volume recombination of these charge carriers in CdS clusters. Moreover, the host porous materials can also provide extra pathways for migration of photoinduced electrons and thus facilitate charge-carrier separation and further increase the photocatalytic efficiency. Another strategy to enhance the photocatalytic activity of CdS is to couple it with other semiconductors.[9-11] The enhancement in the activity of coupled semiconductor system can be ascribed to the favorable band structures in both components that result in effective photoinduced electron and/or hole transfer from one semiconductor to another to minimize electron-hole recombination.

We have adopted the above mentioned strategies and have developed an ultra-stable and highly efficient CdS containing photocatalyst for photo-assisted decomposition of water under visible light illumination. We have previously reported that MCM-48, with its interpenetrating 3-D pores, favour mass transfer kinetics and high dispersion of CdS.[7] However the drawback was the lack of O_2 generation and loss of CdS due to photocorrosion. In this work, CdS was incorporated in Ti-MCM-48 and loaded with co-catalyst RuO_2[12-17] and we realize generation of both H_2 and O_2. The supporting information section contains details of the synthesis. Most importantly, our XPS results indicate *no loss* of *CdS* after the reaction and production of H_2 and O_2 is sustained. For comparison, we also evaluated the activity of Ti-, CdS-, and CdS-Ti-MCM-48.

CdS incorporated in mesoporous materials have been studied before[8, 18], but suffer from the following drawbacks: synthesis of mesoporous materials that are quite time-intensive (up to 7 days), and/or conducted at relatively high temperatures, use of corrosive sulfide as sacrificial agents, use of Pt co-catalyst, very low H_2 yield and absence of O_2, lack of photostability studies, loss of CdS, and formation of CdO after the reaction. To the best of our knowledge, this is the first report of CdS incorporated in mesoporous silica that demonstrates visible light: i) generation of both H_2 and O_2 in the absence of co-catalyst Pt, ii) *no* photocorrosion of CdS even in the *absence* of sulfide or sulfite, and iii) mild conditions for preparation of CdS-Ti-MCM-48 composites. Fig. 1 present the low angle XRD patterns of all studied samples.

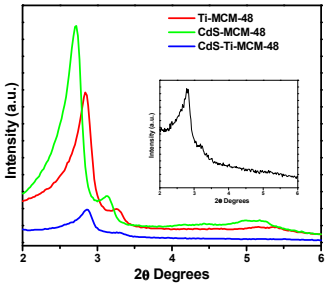

Figure 1. Low angle XRD patterns of studied samples. Inset plot represents the RuO_2-CdS-Ti-MCM-48 sample.

A characteristic Brag reflection due to cubic $Ia\bar{3}d$ symmetry can be perceived in all samples. The strong peaks due to d_{211} and weak d_{220} reflections in the range of 2.5-3.5° demonstrate that the cubic phased mesopore structure was preserved after incorporation of TiO_2, RuO_2, and CdS. Moreover, the peaks, due to d_{321}, d_{400}, d_{420}, and d_{332} in the interval of 4-6° indicate high ordered array of mesopores.[19] Compared to the Ti-MCM-48 sample, CdS-Ti-MCM-48 and RuO_2-CdS-Ti-MCM-48 exhibited

Downloaded by Dalian Institute of Chemical Physics, CAS on 12 March 2013
Published on 27 February 2013 on http://pubs.rsc.org | doi:10.1039/C3CC41362D

less intense peaks. The decrease of peak intensity can be ascribed to the addition of CdS and/or RuO_2 species that cause the lack of the scattering contrast between the pores and pore walls. The high angle XRD patterns of the samples (Fig. S1) show a broad peak at 2θ near 22.5° due to bulk silica. The absence of peaks due to TiO_2, RuO_2, and CdS suggests that these components are highly dispersed in MCM-48. In addition, it is possible that the extremely small size of these species preclude its detection limit of XRD. Nitrogen isotherms (Fig. S2a) show a reversible isotherm of type IV indicating the mesoporous nature. The pore size distribution of the all studied samples exhibits a highly uniform material (Fig. S2b). A summary of the textural properties of the samples are listed in Table 1.

Table 1. Textural properties of all samples.

Material	Si/Ti[a] (mol)	Si/CdS[a] (mol)	Surface Area (m^2g^{-1})	Pore Volume (cm^3g^{-1})	Pore Size (Å)
Ti-MCM-48	47	NA	1312	0.76	19.4
CdS-MCM-48	NA	45	1546	0.82	19.4
CdS-Ti-MCM-48	47	40	1139	0.66	19.3
RuO_2-CdS-Ti-MCM-48	47	42	797	0.58	19.9

[a] Molar ratio in the final product determined by AAS; NA denotes Not applicable.

UV-Vis diffuse reflectance spectroscopy (DRS) is useful in evaluating the local environment of Ti^{4+} and determining the particle size of CdS.

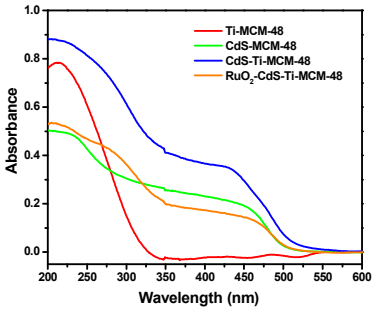

Figure 2. Diffuse reflectance spectra of MCM-48 samples.

Fig. 2 shows the DRS spectra of all samples. In Ti-MCM-48, the strong absorption at ~210 nm is attributed to the ligand to metal charge transfer from O^{2-} to Ti^{4+} in tetrahedral coordination. A broad shoulder at ~270 nm indicates the presence of a fraction of Ti^{4+} in octahedral geometry. The absence of peak near 330 nm suggests no bulk TiO_2 is formed in Ti-MCM-48. Also, the absorption onsets of all Ti-MCM-48 samples is ~350 nm. This indicates that the Ti species are highly dispersed in MCM-48. Meanwhile, the position of adsorption onsets of CdS containing MCM-48 shows a significant blue shift (~500 nm) compared to bulk CdS (~600 nm). The blue shift in CdS absorption onset is due to quantum confinement effects. The band gap energy of the CdS species in CdS-MCM-48 and RuO_2-CdS-Ti-MCM-48 is 2.46 eV and the particle size of CdS is estimated to be ~ 3.4 nm from the Brus equation.[20] Similarly, the band gap energy of CdS in CdS-Ti-MCM-48 is 2.43 eV, and the particle size of CdS is 3.6 nm. The size of CdS is larger than the size of mesopores in Si- and Ti-MCM-48 materials. It is well-documented that small CdS clusters can agglomerate in porous materials including MCM-48 due to quantum tunneling effect.[21] Nitrogen sorption (decrease in pore volume from 0.76 to 0.66 cm^3 on loading CdS) and DRS studies indicate that most of the CdS particles are embedded in the pores of MCM-48 while a small portion of CdS deposited on the external surface of MCM-48 cannot be completely eliminated. X-ray photoelectron spectroscopy (XPS), is a sensitive tool in investigating the surface chemical composition and oxidation state. The XPS plots (Fig. S3) of CdS incorporated samples show peaks at 411.6 and 404.9 eV due to Cd $3d_{5/2}$ and $3d_{3/2}$ with a separation of 6.7 eV which is typical of CdS. The S^{2-} $2p_{1/2}$ and $2p_{3/2}$ peaks appear at 162.4 eV and 161.2 eV and support the formation of CdS. The ratio of S^{2-} to silica was determined to be 0.015 in the sample prior to photocatalytic reaction.

The photocatalytic H_2 and/or O_2 evolution rate and the apparent quantum yield (AQY) are listed in Table 2. Ti-MCM-48 does not generate H_2 and O_2 under visible light. In contrast, all the CdS containing MCM-48 photocatalysts exhibit significant amount of H_2. Compared to the H_2 production generated by CdS-MCM-48 sample (0.22 mmol/h/$g_{catalyst}$), CdS-Ti-MCM-48 gives higher H_2 evolution rate (2.73 mmol/h/$g_{catalyst}$). This remarkable increase in the photocatalytic activity is mainly due to the presence of TiO_2 well dispersed clusters that facilitate transfer of electrons from the c.b. of CdS to TiO_2 in CdS-Ti-MCM-48, thus minimizing electron-hole recombination. Also, the valence band (v.b.) edge of TiO_2 clusters is more positive than the v.b. of CdS and hence, holes in v.b. of CdS cannot diffuse to the TiO_2 v.b. TEM images of CdS-Ti-MCM-48 and RuO_2-CdS-Ti-MCM-48 is shown in Fig. S4 and S5. In RuO_2-CdS-Ti-MCM-48, at low magnifications (Fig. S5a), the cubic phase is seen along with some dark contrasts. At high magnifications (Fig. S5b and Fig. S5c), one can see lattice fringes. Careful examination of the fringes indicates the presence of RuO_2 with d_{200} spacing of 2.43 Å. In addition, lattice fringes due to CdS and TiO_2 are also seen with d_{101} spacing of 3.13 Å and d_{101} spacing of 3.54 Å, respectively. As stated previously, the particle size of CdS estimated from DRS studies is ~ 3.4 nm and the particle size of RuO_2 estimated from TEM studies is ~ 7.5 nm. Results from Energy Dispersive X-ray Spectroscopic (EDS) studies are shown in Fig. S5d, and the distribution of the various elements can be observed. In addition, EDS mapping results indicate the close contact of RuO_2 particles with CdS and TiO_2. The fairly high dispersion of titania in the silica support is also observed.

Table 2. Photocatalytic activities of MCM-48 materials.

Sample	H_2 evolution rate (mmol/h/$g_{catalyst}$)	O_2 evolution rate (mmol/h/$g_{catalyst}$)	AQY [a]
Ti-MCM-48	0	0	0%
CdS-MCM-48	0.22	0	2.9%
CdS-Ti-MCM-48	2.73	0	36.3%
RuO_2-CdS-Ti-MCM-48	0.26	0.13	3.5%

[a] $\mathrm{AQY}(\%) = \frac{\text{the number of evolved H2 molecules} \times 2}{\text{the number of incident photons}} \times 100$

Interestingly, in RuO_2-CdS-Ti-MCM-48, stoichiometric ratio of H_2 (1.56 mmol) and O_2 (0.75 mmol) was achieved by utilizing visible light in the presence of ethanol after 6 h of irradiation. Alcohols such as ethanol have been employed as sacrificial electron donors and higher H_2 yields have been observed since they can be easily photooxidized.[22] We have detected acetaldehyde in our experiments (but have not quantified them) since it is not the focus of our work. Surprisingly, in the presence of a hole transfer agent, *i.e.* in RuO_2-CdS-Ti-MCM-48 we also observe O_2. RuO_2 is a very active catalyst for O_2 evolution because of its low overpotential. In ethanolic solutions, the holes produced in v.b. of CdS can migrate to the surface of the photocatalyst and oxidize ethanol and may also be trapped at the surface by RuO_2 to produce O_2 and it seems that the trapping of

Chemical Communications Accepted Manuscript

This journal is © The Royal Society of Chemistry [year]

View Article Online

Downloaded by Dalian Institute of Chemical Physics, CAS on 12 March 2013
Published on 27 February 2013 on http://pubs.rsc.org | doi:10.1039/C3CC41362D

the holes by RuO_2 is fairly efficient in our system since stoichiometric amounts of O_2 was formed. Thus, the presence of ethanol (sacrificial electron donor) and RuO_2 (low overpotential for O_2 generation) help in the formation of both hydrogen and oxygen. In the presence of pure water under identical conditions, RuO_2-CdS-Ti-MCM-48 forms stoichiometric amounts of H_2 (0.72 mmol/$g_{catalyst}$) and O_2 (0.35 mmol/$g_{catalyst}$) after 6 h of irradiation indicating the role of RuO_2 in generating O_2 but with lower yields as expected as shown in Fig. S6.

To investigate the stability of RuO_2-CdS-Ti-MCM-48, recycling studies were carried out. Fig. 3 shows the photocatalytic H_2 and O_2 rate by RuO_2-CdS-Ti-MCM-48 in ethanol. The results indicate that RuO_2-CdS-Ti-MCM-48 is extremely robust and its photocatalytic activity is sustainable. However, RuO_2-CdS-Ti-MCM-48 shows a significant decrease in the H_2 evolution rate (0.26 mmol/h/$g_{catalyst}$) compared to CdS-Ti-MCM-48. The decrease in H_2 yield is probably due to RuO_2 species that also act as recombination centres of the photogenerated electron-hole pairs.[12] Also, the loading sequence of RuO_2 is prior to CdS into Ti-MCM-48, and thus, the RuO_2 clusters may preclude intimate contact between CdS and TiO_2. In addition, the higher absorbance of CdS-Ti-MCM-48 in comparison to RuO_2-CdS-Ti-MCM-48 may also be a factor responsible for enhanced hydrogen production in CdS-Ti-MCM-48. In order to elucidate the photoinduced charge carriers transfer pathways in CdS-Ti-MCM-48 samples, electron paramagnetic resonance (EPR) study was carried out. Irradiation of CdS by visible light leads to the production of electron-hole pairs. As suggested previously, electrons promoted to c.b. in CdS can be injected into TiO_2. EPR signals were monitored by irradiating the sample with visible light (cut off filter 400 nm) in the presence of glycerol. The EPR spectrum of CdS-Ti-MCM-48 (Fig. S7a) indicates the formation of Ti^{3+} ($g_{\perp}$= 1.958 and $g_{\parallel}$= 1.920) that is

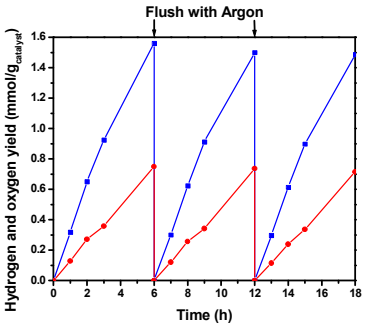

Figure 3. Photocatalytic water splitting over RuO_2-CdS-Ti-MCM-48. Blue squares and Red circles denote H_2 and O_2.

evidence for electron transfer from CdS to TiO_2. A strong signal near g = 2.004 is due to organic radicals formed by the reaction of photogenerated holes with glycerol.[23] A stronger Ti^{3+} peak is found in CdS-Ti-MCM-48 (Fig. S7a) compared to RuO_2 containing sample as seen in EPR plot (Fig. S7b). Hence, efficient transfer of electron from CdS to TiO_2 is prevented and hence H_2 production diminished. Most importantly, XPS studies of CdS-Ti-MCM-48 samples do not show any loss of CdS after the photocatalytic reaction (the ratio of S^{2-} to silica in the spent catalyst remains to be 0.015) even though the reaction was carried out in the absence of sulfide and sulfite as sacrificial agenets. Also, in the XPS plots (Fig. S8) of spent catalysts, CdS show peaks at 411.6 and 404.9 eV due to Cd $3d_{5/2}$ and $3d_{3/2}$ and S^{2-} $2p_{1/2}$ and $2p_{3/2}$ peaks at 162.4 eV and 161.2 eV that indicate the retention of CdS. The intensities of Cd and S in the fresh and spent samples remain virtually unchanged indicating the high stability of CdS after encapsulation in the MCM-48 matrix. Our AAS results also confirm the retention of CdS in RuO_2-CdS-Ti-MCM-48 after long-term photocatalytic reaction and indicate no loss of CdS. The generation of O_2 also indicates that the holes produced in v.b. of CdS does not cause photocorrosion and that oxidation of water occurs as suggested previously.[17]

In conclusion, stoichiometric amounts of H_2 and O_2 can be achieved from photocatalytic decomposition of water by utilizing visible light from RuO_2-CdS-Ti-MCM-48 (1.56 mmol H_2 and 0.75 mmol O_2). The recycling studies of this sample demonstrated a robust and ultra-stable photocatalyst with no loss of CdS even in the absence of sulfide/sulfite as sacrificial agents. The results suggest that encapsulation of CdS, presence of well-dispersed titania, and use of RuO_2 in RuO_2-CdS-Ti-MCM-48 results in the first photocatalyst supported mesoporous silica that generates stoichiometric H_2 and O_2 and most importantly eliminates photocorrosion of CdS completely. Such strategies may provide opportunities for development of novel photocatalysts with enhanced efficiencies for solar energy conversion.

Thanks are due to NSF–CHE–0722632, NSF–EPS–0903804, DE–EE0000270, and SD NASA-EPSCOR NNX12AB17G. The work at the Center for Nanoscale Materials was supported by the U.S. DOE, under contract DE-AC02-06CH11357.

Notes and references

*[a] *Department of Chemistry, University of South Dakota, Vermillion, SD 57069, USA.E-mail: Ranjit.Koodali@usd.edu*
[b] *PhotoCatalytic Synthesis Group, University of Twente, The Netherlands*
[c] *Center for Nanoscale Materials, and Chemical Sciences and Engineering Division, Argonne National Laboratory, Argonne, Illinois 60439 USA.*

Supplementary information available: See DOI: 10.1039/b000000x

1. A. Fujishima and K. Honda, *Nature*, 1972, **238**, 37-38.
2. A. Kudo and Y. Miseki, *Chemical Society Reviews*, 2009, **38**, 253-278.
3. X. Chen, S. Shen, L. Guo and S. S. Mao, *Chemical Reviews*, 2010, **110**, 6503-6570.
4. M. Ashokkumar, *International Journal of Hydrogen Energy*, 1998, **23**, 427-438.
5. M. D. Hernandez-Alonso, F. Fresno, S. Suarez and J. M. Coronado, *Energy Environ. Sci.*, 2009, **2**, 1231-1257.
6. T. Inoue, T. Watanabe, A. Fujishima, K.-i. Honda and K. Kohayakawa, *Journal of The Electrochemical Society*, 1977, **124**, 719-722.
7. R. Peng, D. Zhao, J. Baltrusaitis, C.-M. Wu and R. T. Koodali, *RSC Advances*, 2012, **2**, 5754-5767.
8. S. Y. Ryu, W. Balcerski, T. K. Lee and M. R. Hoffmann, *The Journal of Physical Chemistry C*, 2007, **111**, 18195-18203.
9. Y. Chen, L. Wang, G. Lu, X. Yao and L. Guo, *Journal of Materials Chemistry*, 2011, **21**, 5134-5141.
10. T. Kida, G. Guan, Y. Minami, T. Ma and A. Yoshida, *Journal of Materials Chemistry*, 2003, **13**, 1186-1191.
11. H. Yan, J. Yang, G. Ma, G. Wu, X. Zong, Z. Lei, J. Shi and C. Li, *Journal of Catalysis*, 2009, **266**, 165-168.
12. D. Duonghong, E. Borgarello and M. Graetzel, *Journal of the American Chemical Society*, 1981, **103**, 4685-4690.
13. H. Kato, K. Asakura and A. Kudo, *Journal of the American Chemical Society*, 2003, **125**, 3082-3089.
14. A. Iwase, H. Kato and A. Kudo, *Chemistry Letters*, 2005, **34**, 946-947.
15. M. Hara, C. C. Waraksa, J. T. Lean, B. A. Lewis and T. E. Mallouk, *The Journal of Physical Chemistry A*, 2000, **104**, 5275-5280.
16. A. Ishikawa, T. Takata, J. N. Kondo, M. Hara, H. Kobayashi and K. Domen, *Journal of the American Chemical Society*, 2002, **124**, 13547-13553.
17. K. Kalyanasundaram, E. Borgarello, D. Duonghong and M. Grätzel, *Angewandte Chemie International Edition in English*, 1981, **20**, 987-988.
18. T. Hirai, H. Okubo and I. Komasawa, *J. Phys. Chem. B*, 1999, **103**, 4228-4230.
19. B. Boote, H. Subramanian and K. T. Ranjit, *Chemical Communications*, 2007, 4543-4545.
20. M. L. Steigerwald and L. E. Brus, *Annual Review of Materials Science*, 1989, **19**, 471-495.
21. N. Herron, Y. Wang, M. M. Eddy, G. D. Stucky, D. E. Cox, K. Moller and T. Bein, *Journal of the American Chemical Society*, 1989, **111**, 530-540.
22. U. Pal, S. Ghosh and D. Chatterjee, *Transition Metal Chemistry*, 2012, **37**, 93-96.
23. R. Peng, D. Zhao, N. M. Dimitrijevic, T. Rajh and R. T. Koodali, *Journal of Physical Chemistry: C*, 2012, **116**, 1605-1613.

Chemical Communications Accepted Manuscript

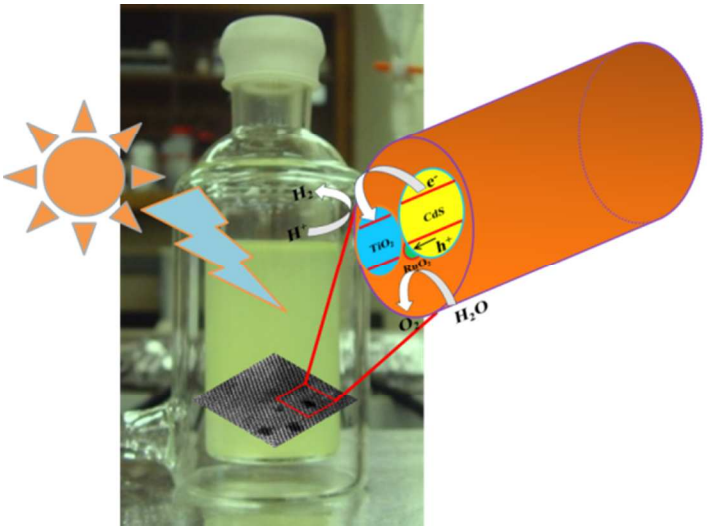

Downloaded by Dalian Institute of Chemical Physics, CAS on 12 March 2013
Published on 27 February 2013 on http://pubs.rsc.org | doi:10.1039/C3CC41362D

Chemical Communications Accepted Manuscript

This journal is © The Royal Society of Chemistry [year]